# Modulating Membrane Properties: The Effect of Trehalose and Cholesterol on a Phospholipid Bilayer

**Manolis Doxastakis**

*Department of Chemical and Biological Engineering, University of Wisconsin, Madison, Wisconsin 53706*

**Amadeu K. Sum**

*Department of Chemical Engineering, Virginia Polytechnic Institute and State University, Blacksburg, Virginia 24061*

**Juan J. de Pablo***

*Department of Chemical and Biological Engineering, University of Wisconsin, Madison, Wisconsin 53706*

*Received: August 26, 2005; In Final Form: October 24, 2005*

The protective properties of trehalose on cholesterol-containing lipid dipalmitoylphosphatidylcholine (DPPC) bilayers are studied through molecular simulations. The ability of the disaccharide to interact with the phospholipid headgroups and stabilize the membrane persists even at high cholesterol concentrations and restricts some of the changes to the structure that would otherwise be imposed by cholesterol molecules. Predictions of bilayer properties such as area per lipid, tail ordering, and chain conformation support the notion that the disaccharide decreases the main melting transition in these multicomponent model membranes, which correspond more closely to common biological systems than pure bilayers. Molecular simulations indicate that the membrane dynamics are slowed considerably by the presence of trehalose, indicating that high sugar concentrations would serve to avert possible phase separations that could arise in mixed phospholipid systems. Various time correlation functions suggest that the character of the modifications in lipid dynamics induced by trehalose and cholesterol is different in the hydrophilic and hydrophobic regions of the membrane.

## I. Introduction

The stabilizing effect of sugars on biological membranes has been well-established by several studies.[1−8] Trehalose, a nonreducing dissacharide of glucose, has been isolated from freeze- and desiccation-tolerant organisms such as baker's yeast, resurrection plants, and bacteria, where it occurs at relatively high concentrations (as much as 20% of the dry weight).[9−11] Trehalose has subsequently found significant applications in the food, biomedical, pharmaceutical, and cosmetics industries.

The mechanisms through which sugars stabilize liposomes or cells are considered to be a direct substitution of water molecules in the outer hydrophilic part of the membrane (water replacement hypothesis) and the formation of a glass that prevents fusion and reduces dehydration-induced stresses (vitrification).[12−14] These two mechanisms of action are not mutually exclusive, and both require that a certain amount of sugar be partitioned in the proximity of the phospholipid headgroups. Experimental studies on model monolayers or membranes composed of a single phospholipid species support the existence of specific interactions between the membrane constituents and trehalose molecules (and a concomitant enhancement of trehalose in the immediate vicinity of the polar lipid headgroups).[9,15−19] The replacement of water by trehalose molecules in the hydrophilic part of dry membranes could in principle be directly connected to changes in the phase behavior of the lipid membranes. In dipalmitoylphosphatidylcholine (DPPC) membranes dried in the presence of trehalose, the main gel-to-liquid crystalline transition is depressed from 110 °C to 24 °C.[12] Avoiding phase transitions is of vital importance in lyophilization, since such effects can lead to leakage across the bilayer membrane.[20]

Recent molecular simulation studies from our group have provided new insights into the stabilizing role of sugars.[21−23] The presence of specific interactions between sugars (trehalose or sucrose) and a DPPC bilayer has been studied in atomistic detail.[24] Several of the main findings from our simulations have also been supported by subsequent studies from other research groups.[25,26] Note, however, that while the local enhancement of trehalose in the headgroup region of simple phospholipid bilayers has been confirmed by both simulation and experimental studies, important aspects of this effect (e.g., changes in the area per lipid, ordering of the lipid tails, local dynamics of the membrane) have not been fully addressed. More importantly, biological membranes are composed of a variety of constituents, and past studies have postulated that trehalose provides additional stabilization by maintaining their lateral organization.[10,27] A recent study of the phase behavior of freeze-dried phospholipid−cholesterol mixtures stabilized with trehalose has shown that the phase separation of lipidic components is limited by the presence of the sugar.[28]

A considerable research effort is currently aimed at exploiting the stabilizing properties of disaccharides in various technological applications. Trehalose has been used in experiments with human pancreatic islets,[29,30] fibroblast cells,[31,32] T-lymphocyte cells,[33,34] blood platelets,[35−37] fetal skin,[38] human embryonic stem cells,[39] and red blood cells.[40] Eukaryotic plasma cell membranes are complex multicomponent systems. A common constituent in mammalian cell membranes is choles-

* Electronic address: depablo@engr.wisc.edu.

10.1021/jp054843u CCC: $30.25 
Published on Web 11/25/2005

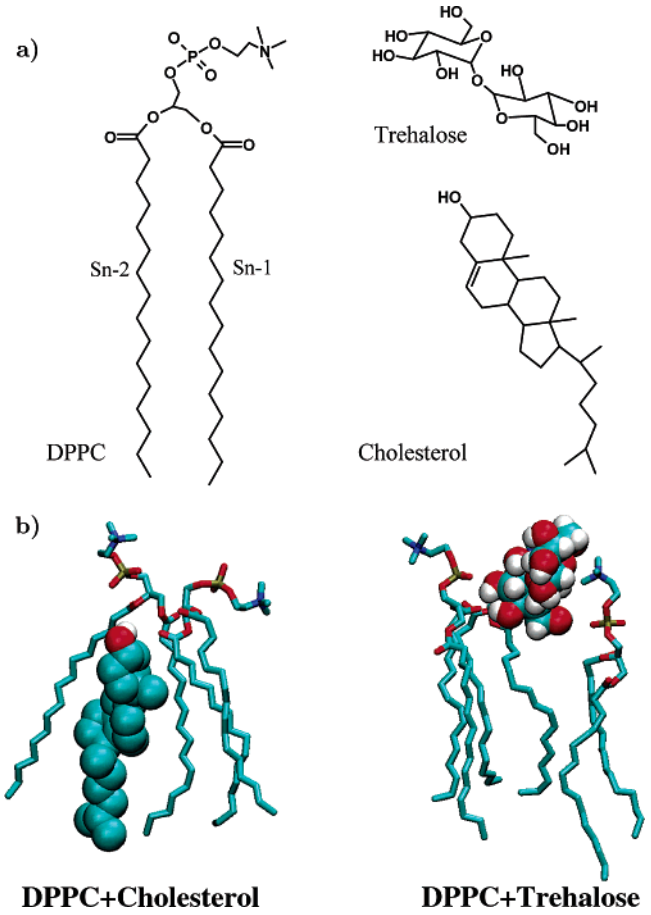


**Figure 1.** (a) Chemical structures of DPPC, trehalose, and cholesterol. (b) Interactions of cholesterol and trehalose with neighboring DPPC molecules in a lipid bilayer as probed in the liquid crystalline phase.

terol, which occurs at contents as high as 50 mol %. Human erythrocytes, for example, include a mixture of lipids and 45 mol % cholesterol.[41]

Past molecular simulations of trehalose bilayer systems have not considered the effects of cholesterol. Note, however, that the effect of cholesterol in pure model membranes (i.e., in the absence of trehalose) has been examined by several research groups. A number of experimental findings have been confirmed, and valuable new insights have been gained through studies of cholesterol−DPPC and cholesterol−DMPC (dimyristoylphosphatidylcholine) bilayers.[42−55] Cholesterol resides in the hydrophobic part of a lipid bilayer and, among many effects, alters the packing, free area, diffusion, and permeability of the cell membrane.

The growing use of disaccharides in the stabilization of mammalian cells directs us to investigate multicomponent, cholesterol-containing membranes in the presence of sugars. In this work, the combined effect of a protectant molecule and a rigid component on membrane behavior are probed using atomistic simulations of mixed DPPC−cholesterol bilayers in the presence of α,α-trehalose (Figure 1a). The results reported here extend our knowledge on lipid bilayers and provide an understanding of the changes inflicted on cell membranes by two different mechanisms: a solute that preferentially interacts with the hydrophilic phosphorus headgroups and a component that resides between the lipid tails and affects the hydrophobic part of the membrane. The changes induced by these two components in the thermodynamics and dynamics of cell membranes can be considerably different. Trehalose not only depresses the gel-to-liquid crystalline transition of DPPC, but

**TABLE 1: Composition of Simulated Lipid Bilayer Systems[a]**

| system | DPPC | water | cholesterol[b] | trehalose[c] | simulation time[d] (ns) 400/350/323 K |
|---|---|---|---|---|---|
| A1 | 128 | 4336 | | | 20.1/22.9/27.2 |
| A2 | 128 | 4336 | | 8 (3.5%) | 20.1/22.6/29.5 |
| A3 | 128 | 3656 | | 42 (21.8%) | 20.4/23.2/30.0 |
| B1 | 128 | 4336 | 16 (12.5%) | | 21.0/22.4/30.8 |
| B2 | 128 | 4336 | 16 | 8 | 22.1/22.0/28.2 |
| B3 | 128 | 3656 | 16 | 42 | 22.6/22.6/28.0 |
| C1 | 128 | 3656 | 48 (37.5%) | - | 21.7/23.8/33.0 |
| C2 | 128 | 4336 | 48 | 8 | 21.0/21.1/28.2 |
| C3 | 128 | 3656 | 48 | 42 | 21.7/21.6/26.8 |

[a] The abbreviations listed in the first column are used for brevity throughout the text (letters correspond to different cholesterol content, while numbers correspond to concentrations of trehalose in the system). [b] Concentration in parentheses given in %mol of the lipid content. [c] Concentration in parentheses given in wt % on lipid-free basis. [d] The final configuration of each simulation was used as starting point for the next lower temperature.

in dry mixtures, it is believed to lead to a new type of liquid crystalline phase, the $\lambda$-phase,[16] with highly disordered lipid acyl chains and excluded fast long-axis diffusion. Cholesterol enhances the lipid tail orientation in the liquid crystalline phase and disrupts ordering in the gel phase (Figure 1b). In contrast to the temperature shift caused by trehalose, the phase transition as probed by differential scanning calorimetry broadens by increasing the cholesterol content, and the enthalpy of the transition decreases and eventually disappears at concentrations above 25 mol %.[56] Therefore, apart from significant technological aspects, the concurrent effects of trehalose and cholesterol in a lipid bilayer represent an intriguing model system for detailed molecular studies.

## II. Simulation Methods and Details

Molecular dynamics simulations were performed on hydrated bilayer systems containing 128 DPPC molecules and 3 different concentrations of trehalose and cholesterol at 400, 350, and 323 K. The trehalose concentration is similar to that employed in our previous study of pure (cholesterol-free) bilayers.[24] Details of the molecular systems are presented in Table 1, together with the nomenclature used throughout the text.

The interaction parameters for the lipids were assembled from the GROMOS force field[57] for the headgroups of DPPC and the NERD force field[58−60] for the aliphatic tails, consistent with our previous study of lipid bilayers exposed to trehalose. A united atom model is also employed for cholesterol, taken from http://www.gromacs.org/topologies/uploaded_molecules/cholesterol.tgz.[61] Disaccharide interactions are described by the OPLS[62] parameters, and the SPC model is adopted for water.[63]

Simulations were performed using the GROMACS molecular dynamics software.[64,65] A leapfrog integration algorithm with a time step of 2 fs was employed. This choice of time step was made feasible by constraining all bond lengths to reference values by the LINCS algorithm.[66] The nonbonded interactions were accounted for using a twin-range cutoff scheme. Within 10 Å, interactions were evaluated at every time step on the basis of a pair list recalculated every 10 steps. Intermediate-range interactions from 10 to 12 Å were calculated simultaneously with each pair list update and assumed constant in between. Lennard-Jones interactions were cut off at 12 Å, where long-range electrostatics were handled using the smooth particle-mesh Ewald method[67] with a grid spacing of 1 Å, a real space cutoff at 10 Å, and a Gaussian width of 0.312 $Å^{-1}$.

The temperature and the pressure were kept constant using the weak coupling technique[68] with correlation times $\tau_T = 0.1$

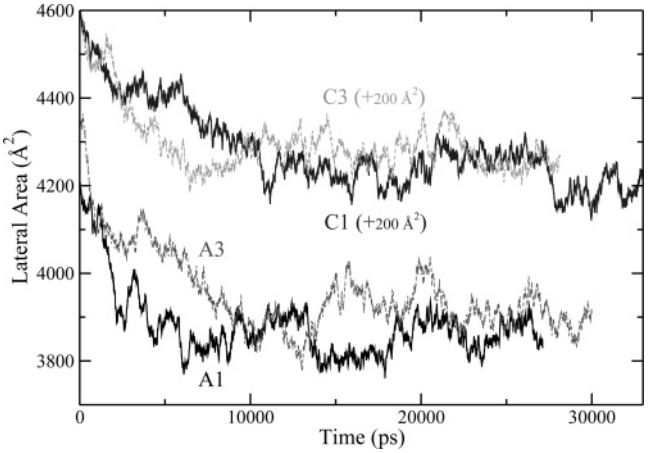


**Figure 2.** Evolution of the lateral area of selected systems as a function of simulated time at 323 K. Curves describing the cholesterol-containing systems (C1 and C3) have been shifted by +200 Å² for clarity. After an initial equilibration period of up to 10 ns, the molecular systems present fluctuations around the average value at the specific temperature.

ps and $\tau_P = 2.0$ ps for temperature and pressure, respectively. Pressure was independently coupled in three directions to an ambient pressure of 1 bar with a compressibility of $0.46 \times 10^{-4}$ $bar^{-1}$, thereby allowing the area of the bilayer and the distance between the interfaces to fluctuate independently.

The starting point of all systems was an ordered configuration of 128 lipids separated into 2 layers with their centers of mass positioned in a lattice arrangement. The bilayer was aligned such that it lies in the $x-y$ plane, i.e., the bilayer normal is parallel to the $z$ axis. Cholesterol molecules were placed at random positions between the lipids, equally divided between the two layers. The main axis of each inserted cholesterol was parallel to the $z$ axis, with the hydroxyl group in the proximity of the lipid carbonyl groups. The water was placed in two layers adjacent to the phospholipid headgroups, and the sugar was arranged in a layer in the middle of the aqueous region. Such a spatial distribution was chosen as an initial structure to avoid imposing any disaccharide−lipid interactions in the starting configuration.

Trehalose diffusion in aqueous solutions at low temperatures is relatively slow,[21−23] thereby posing significant challenges for the creation of equilibrium structures, particularly at low temperatures.[26] To overcome the computational demands of modeling a variety of trehalose and cholesterol concentrations at biological relevant conditions (i.e., 323 K), consistent with previous studies, higher temperatures were first employed to generate initial configurations.[24,25] Systems were first equilibrated at a high temperature of 450 K, with no positional restraints, where all components are mobile enough to adjust to their favorable configuration. During this equilibration period, the lipids do not exhibit lateral order, but they retain their bilayer arrangement. Subsequent simulations were performed at 400, 350, and 323 K; the final configuration of each simulation was submitted as a starting point for the next lower temperature. After a preequilibration of up to 10 ns, data were acquired every 10 ps for at least 20 ns to ensure sufficent sampling of both structural and dynamic quantities. Properties were calculated only when the thermodynamic properties monitored exhibited normal fluctuations around their average values, as shown in Figure 2 for the lateral area of four of the nine systems studied (A1, A3, C1, and C3) at the lowest temperature (323 K) considered in this work.

To extract the short-time dynamic behavior of the systems, simulations were also performed for each system, at each temperature, for 20 ps with data collected every 20 fs. Since the short runs remain in the vicinity of the initial structure because of limited sampling, the starting configuration was chosen from the trajectory of the long runs so that it corresponds to a state of equilibrium (e.g., the lateral dimension of the bilayer equal to the average of the long *NPT* simulations).

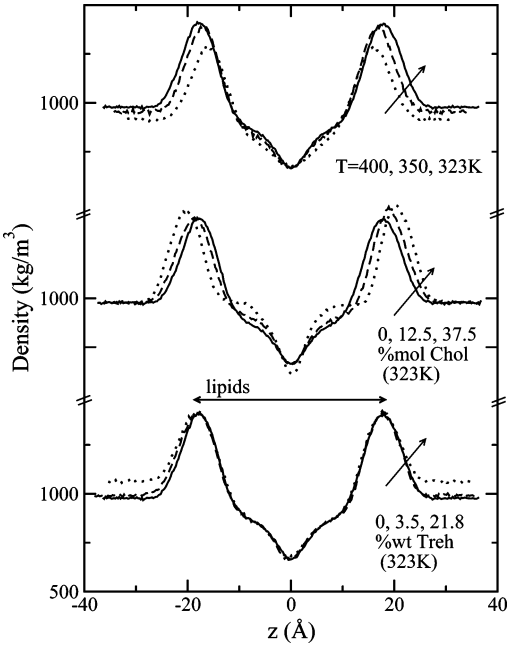


**Figure 3.** Temperature, cholesterol, and trehalose effect on the density profile along the membrane normal. Top profile corresponds to system A1 (see Table 1) at 400 K (dotted line), 350 K (dashed), and 323 K (continuous); middle profile to A1 (continuous), B1 (dashed), and C1 (dotted) at 323 K; and bottom profile to A1 (continuous), A2 (dashed), and A3 (dotted) at 323 K, respectively. All profiles are calculated from the simulation trajectories by removing the center of mass motion of the lipids along the $z$ direction.

## III. Results and Discussion

**A. Structure of Membrane.** We first examine the structure of the bilayer along the membrane normal as affected independently by each of the three factors considered in our simulations: temperature, cholesterol, and trehalose concentration. Figure 3 displays the density profile along the $z$ direction (membrane normal) for each of the three cases. For the temperatures considered in this work, all of our pure bilayer systems sample the liquid crystalline phase and the effect of temperature is moderate. The density of the aqueous phase increases as the temperature is lowered, and a distinct change in the separation of the main two density peaks is observed. These two peaks are associated with the location of the phospholipid headgroups of each layer, and their location is indicative of the swelling of lipid bilayers as the main melting transition is approached. This effect has been well-documented in experimental work.[69−72] In the hydrophobic regime, a slight change in the profile is detected, with the density showing signs of a non-monotonic decrease toward the center of the bilayer ($z = 0$). While the effect of temperature in the lipids tail regime is moderate, the inclusion of cholesterol alters the profile significantly. The decrease is distinctly non-monotonic, with the clear development of a plateau at the higher cholesterol concentrations, as also found by other simulation studies.[53,54] A thickening of the bilayer is also observed, as shown by the displacement of the main two peaks. In contrast to the effect of temperature, the density of the aqueous phase is hardly affected.

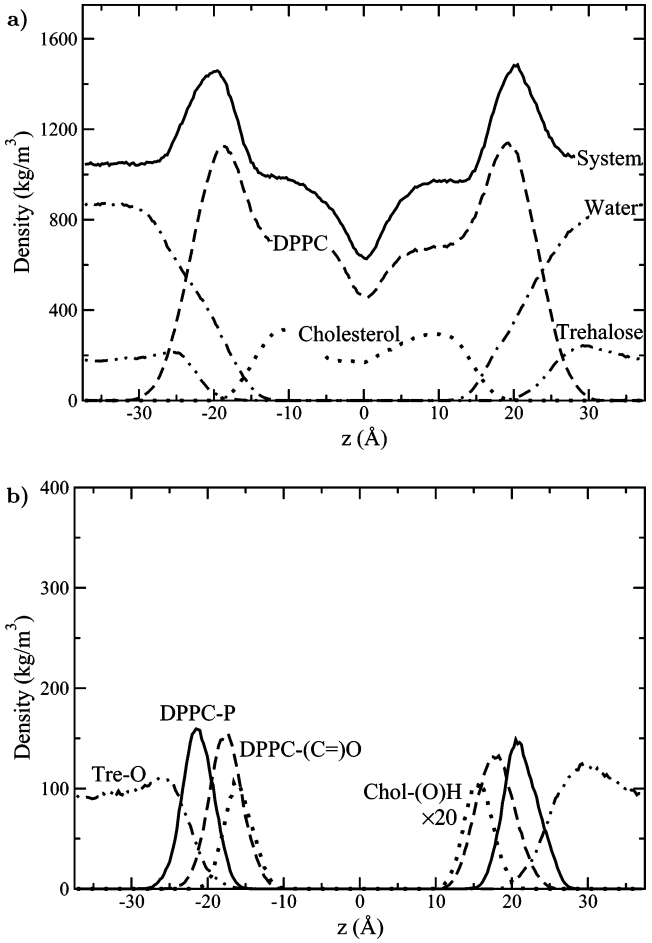


**Figure 4.** (a) Density profile of fully hydrated DPPC (dashed line) in the presence of trehalose (dashed−double dotted line) and cholesterol (dotted line) as calculated at 323 K for system C3. The water region is shown by the dashed−dotted line. (b) Partial density profile for trehalose oxygens (dashed−double dotted line), DPPC−phosphorus (continuous line), DPPC−carbonyl oxygens (dashed line), and cholesterol hydroxyl hydrogen (dotted line) for the same system.

An apparent change in the water regime is achieved by the inclusion of trehalose. The last density profile demonstrates that the sugar increases the density of the aqueous region and slightly broadens the two main peaks.

The same main effects observed in the above cases are also found by examining the structure of a system (C3) in the presence of both cholesterol and trehalose. Figure 4a presents the density profile for the system containing the highest amount of cholesterol and trehalose, at 323 K. All major features are still observed and analyzed by plotting each component separately. Cholesterol is distributed in the hydrophobic area and affects the membrane structure. Trehalose partitions preferentially to the headgroup region, where it increases the local density considerably. A small maximum in the trehalose distribution is observed in the proximity of the interface at all temperatures studied in this work. There is no regime along the membrane normal where cholesterol molecules coexist with trehalose to any significant extent.

The densities of trehalose oxygens, lipid phosphorus atoms, lipid carbonyl oxygens, and cholesterol hydroxyl hydrogen are plotted in Figure 4b. The location of each species is a direct result of their respective interactions with specific lipid groups. The sugar binds mainly to the headgroups and, to a smaller extent, to the lipid carbonyl oxygens.[24] In contrast, cholesterol binds mainly to the carbonyl groups and, to a smaller extent, to

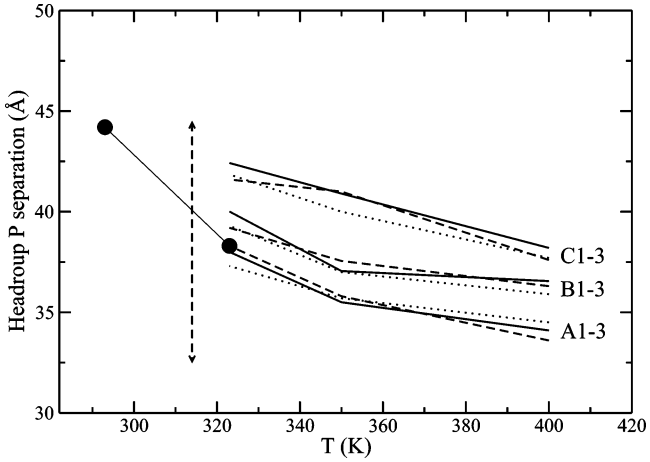


**Figure 5.** Thickness of the bilayer as defined by the headgroup phosphorus separation of the two leaflets. Continuous lines correspond to trehalose-free systems; dashed and dotted lines correspond to intermediate and high sugar concentrations, respectively. Filled circles are experimental data from the literature[73] for cholesterol-free DPPC bilayers before and after the melting transition (indicated by the vertical dashed line).

the lipid headgroups (and to a different extent than in the case of shorter lipids, as DMPC).[53,52] The above findings are also shown graphically in Figure 1b. While these specific interactions have been reported in lipid−cholesterol and lipid−trehalose systems, they persist in the three-component systems considered in this work. The two peaks corresponding to the lipid phosphorus distribution are well-resolved and provide a means of defining the bilayer thickness. The *z* coordinate of their maxima is approximately equal to the location of the density maxima shown in Figure 3.

The thickness of the bilayer, as extracted from the maxima of the headgroup phosphorus atoms, is plotted in Figure 5. The three sets of lines (A, B, and C) correspond to different cholesterol content; different line styles are chosen according to trehalose concentration. The vertical dashed line is drawn to indicate the main melting transition temperature, as measured in experiments with pure DPPC bilayer membranes. Filled circles correspond to experimental data from the literature[73] for the liquid crystalline and the gel phase for cholesterol-free DPPC membranes. There is excellent agreement between the predictions of simulations and experiment at 323 K. The temperature effect is manifested by a moderate increase of the thickness of the bilayer. The inclusion of cholesterol induces a drastic change in the thickness and is consistent with X-ray diffraction studies.[74] Any change of thickness due to the presence of the sugar was not detected within the statistical accuracy of our simulations, except for the system with the highest cholesterol and trehalose content (C3), where a systematic trend toward lower values is observed.

Another property that is often used to describe the thermodynamic state of a lipid bilayer is the area per lipid. For unicomponent lipid bilayers, this property is easily derived from the lateral dimensions of the system divided by the number of lipids in each layer (64 in our systems). In the presence of trehalose, the area per lipid is calculated in the same manner, but the inclusion of cholesterol poses the problem of knowing the "area" of a cholesterol molecule.[54] A range of values has been used in the literature, from 26 to 39 Å$^2$. To obtain an accurate value for the lateral area occupied by a cholesterol molecule in a lipid bilayer, the effect of temperature and sterol concentration should be explored. This is not the main subject of our study; furthermore, even a detailed analysis in terms of

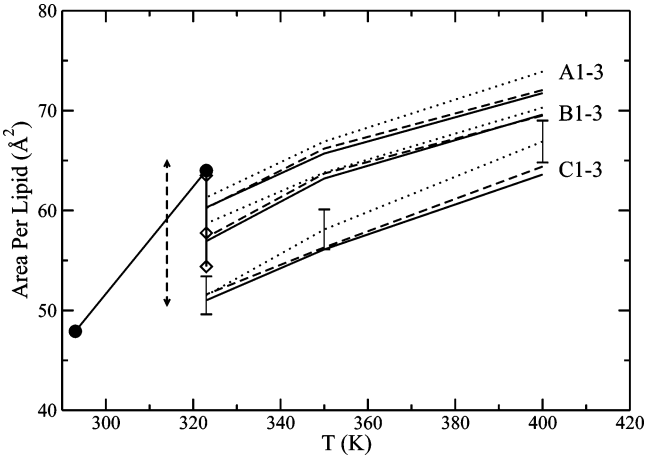


**Figure 6.** Area per lipid for the nine systems studied in this work, as shown by the three sets of lines. Filled circles correspond to experimental data[73] for cholesterol-free bilayers. Open diamonds correspond to a literature simulation study of a DPPC-bilayer at the same cholesterol content.[49] Error bars for one system (C3) are given to evaluate the effect of different estimates for the cholesterol molecular area.

Voronoi tessellation can result in molecular areas having little quantitative meaning.[54] We therefore adopt a constant value of 32 Å$^2$ for our analysis[43] and use other limiting values (26 and 39 Å$^2$) to define an error estimate for our area-per-lipid predictions. The results of our studies are summarized in Figure 6. Filled points correspond to selected experimental estimates in the 2 phases, extracted from derived analysis of a wide range of values reported in the literature.[73] Our calculations underestimate the experimental data by approximately 3.5%. However, most of the simulation studies reported in the literature provide estimates below the experimental value of 64 Å$^2$ and are often in worse agreement with experiment than the predictions reported in this work.[25] The dependence of the area per lipid on cholesterol content can be inferred by following the variation of the continuous lines (A, B, and C). Using a constant value for the cholesterol molecular area can introduce a significant error, as suggested by the error bars (only shown for the systems with highest cholesterol content, C3, for clarity, as calculated for the two limiting values of molecular area of cholesterol); nevertheless, a condensing effect is apparent in the substantial decrease of the area per lipid determined by any of the above-mentioned estimates for the sterol molecular area. At all temperatures, in the liquid crystalline phase the inclusion of cholesterol at high molar ratios alters significantly the packing in the membrane, in agreement with results from literature simulations. Open diamonds correspond to values extracted from results by Hofsäss et al. using a large system of 1024 lipids but a simple cutoff for electrostatic interactions;[49] these values are in good agreement with our predictions for all 3 concentrations of cholesterol. Despite the statistical error involved in the calculations, the presence of trehalose at the concentrations of our simulations has a minor effect that persists at all temperatures and systems studied. A slight increase of the area per lipid is apparent, as shown by the dashed and dotted lines (intermediate and high concentrations, respectively). Although the changes are not large, it is important to emphasize that the modifications to the bilayer structure induced by the sugar persist in cholesterol-containing membranes.

The induced changes in the bilayer structure can also be evaluated more definitely (without adopting values for the cholesterol area) through the gauche population of dihedral angles in the lipid tails. The gauche fraction was determined

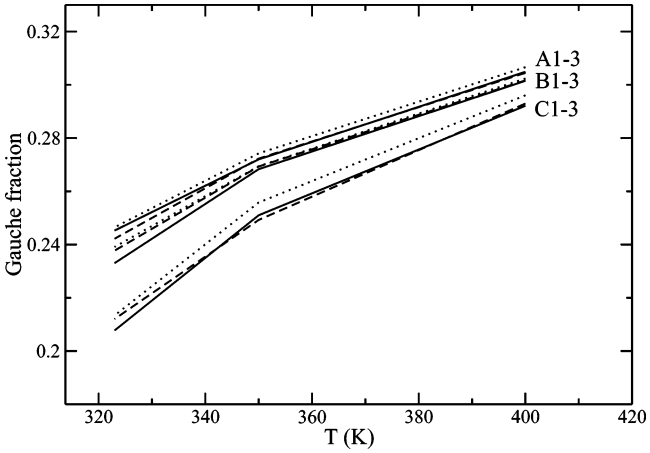


**Figure 7.** Gauche fraction of lipid tails as a function of temperature, cholesterol, and trehalose concentration for all systems studied in this work.

by integrating the normalized torsion angle distribution of all angles in both lipid tails from −120° to 120°. The calculated values are plotted in Figure 7, using the same notation as in previous figures. For trehalose-free systems, the predicted values are in agreement with previously reported simulation results.[49] The changes in the area per lipid induced by cholesterol and trehalose are also bourn out by the conformations of the lipid tails. An increased gauche fraction is observed for the highest concentration of sugar. Cholesterol, as expected, induces a significant increase of the trans fraction. A competition of effects arises, and the disaccharide presence is felt even at the highest sterol concentration.

To explore the hydrophobic part of the membrane in more detail, the orientation of the lipid tails as a function of position along the chain was analyzed for all systems at the three temperatures considered in this work. In lipid bilayers, the orientation of tails is commonly expressed through the deuterium-order parameter ($S_{CD}$),[75] a property measured experimentally by NMR methods[76]

$$S_{CD} = \frac{1}{2}(3\langle \cos^2 \theta_{CD} \rangle - 1) \qquad (1)$$

where $\theta_{CD}$ is the angle between a carbon−deuterium bond at a particular carbon position along the tail and the membrane normal. A value for $S_{CD}$ of −0.5 corresponds to parallel alignment of the lipid tails with the membrane normal. Figure 8 presents the results of our simulations for one of the two lipid tails (Sn−1) at two temperatures, 323 and 400 K. By examining first the pure bilayer systems (system A1) at 400 and 323 K, it is clear that as the temperature is reduced the lipid chains orient more parallel to the membrane normal. At high temperatures, moving toward the end of the tail, a higher degree of disorder is found; at lower temperatures, however, a plateau region appears. The development of a constant-orientation part of the lipid tails at values of approximately 0.2 is consistent with results of NMR experiments reported in the literature.[77] The inclusion of cholesterol molecules in the hydrophobic part of the membrane has a considerable impact on the orientation of the tails in the liquid crystalline phase. A drastic increase of order is apparent from the continuous lines in the figure, moving from the pure bilayer (system A) to the higher cholesterol content (system C). At the lowest temperature, the effect is amplified in the middle of the lipid tails, in the region of the membrane where the rigid rings of the sterol reside. Our data are in good agreement with literature studies for lipid−cholesterol systems[54] for both the Sn−1 and the Sn−2 lipid tails.

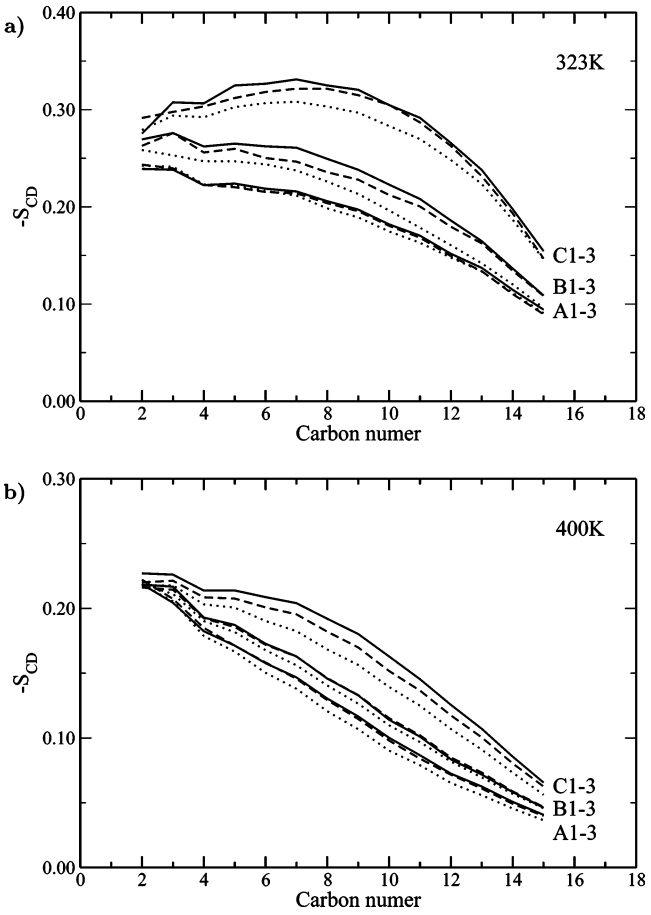


**Figure 8.** (a) Deuterium order parameter $S_{CD}$ as a function of the carbon position along the Sn−1 lipid chain at 323 K for all systems studied. (b) Deuterium order parameter $S_{CD}$ as a function of the carbon position along the Sn−1 lipid chain at 400 K for all systems studied.

Upon addition of trehalose to the aqueous phase, some of the sugar molecules intercalate with the membrane headgroups, with a concomitant increase of the area per lipid. This small expansion of the lipids modifies the degree of lipid tail orientation, as evidenced by the deuterium order parameter. For pure lipid bilayers, the effect is again minor, in agreement with our findings for the area per lipid. We find that the disruption of lipid order by the sugar is more evident in the systems that contain a considerable amount of cholesterol. While the disaccharide partitions preferentially to the polar headgroup region, the interactions between the sugar molecules and the carbonyl groups compete against the condensing effect of cholesterol and diminish the change of the structure imposed by the latter. Despite the fact that the predicted profiles are more accurate at high temperatures, where sampling of statistically distinct conformations is more efficient, qualitatively the same physical picture is obtained at all temperatures. Thus, solutions of trehalose at low and moderate concentrations modify slightly the structure of hydrated bilayers, and their effect in systems containing considerable amounts of sterols is clearly significant.

**B. Dynamics of Membrane.** The membrane in the liquid crystalline phase possesses the properties of a fluid along the lateral dimension. The molecular motion of lipidic components along the $x-y$ plane is expressed through a self-diffusion coefficient $D$, calculated from the mean square displacement of the molecules

$$D = \lim_{\Delta t \to \infty} \frac{\langle [r(t + \Delta t) - r(t)]^2 \rangle}{4\Delta t} \qquad (2)$$

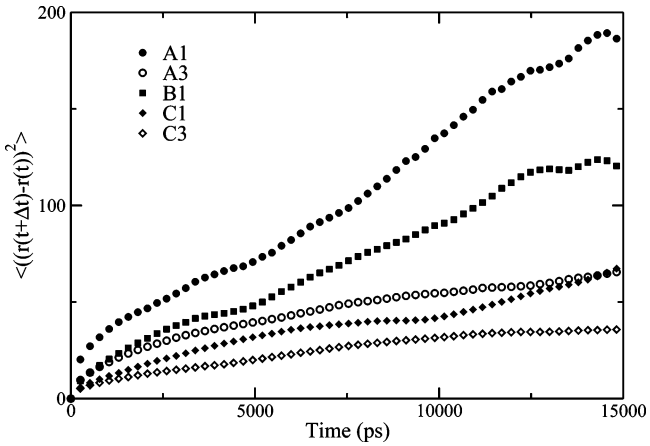


**Figure 9.** Mean square displacement of lipids along the lateral dimension of the bilayer for select systems at 323 K. Filled symbols correspond to three different cholesterol contents; open symbols correspond to systems with and without cholesterol in the presence of trehalose.

Mean square displacements along the lateral dimension of the bilayer are plotted for selected systems in Figure 9. It can be seen that both cholesterol and trehalose reduce the molecular mobility of the lipids considerably. The $D$ values extracted from linear fits for the trehalose-free systems (A1, B1, and C1) are $2.9 \cdot 10^{-7}$, $1.9 \cdot 10^{-7}$, and $9.4 \cdot 10^{-8}$ cm$^2$/s, in excellent agreement with data reported in the literature.[49] In the presence of disaccharides, the diffusive regime is not attained in our simulations, and accurate estimates of $D$ cannot be obtained (the mean displacement during the length of our simulations is rather short, approximately 10 Å). It is clear, however, that even systems containing high amounts of cholesterol are susceptible to further decrease of their diffusion coefficients by addition of trehalose, as shown by the mean square displacement of the lipids in systems C1 and C3. On the basis of experimental results, it has been postulated that, apart from maintaining the separation of membrane molecules, sugars can maintain the lateral organization of membrane constituents by binding to the phospholipids headgroups, thereby reducing any tendency of a mixed system to phase separate (or of a spatially organized system to mix).[10,27,28] Changes in lateral organization would disrupt the structure of cell membranes and enhance the possibility of leakage and cell death during lyophilization procedures. Our simulation results support this additional protective mechanism of trehalose by predicting a reduced molecular mobility of the membrane constituents, an effect that is expected to be more pronounced at even higher trehalose concentrations, where long-range lateral mobility might be suppressed.

As indicated above, the sugar and the sterol reside in different parts of the membrane. It is therefore anticipated that, although both appear to reduce the molecular mobility of the lipids, the resulting changes could be different along the bilayer normal. To gain insight into the local effect of the presence of trehalose and cholesterol, the dynamics of the headgroups and tails have been examined separately. The mobility of the headgroups can be extracted by the reorientation of the unit vector along the direction defined from the phosphorus atom to the nitrogen atom of the same DPPC molecule. The autocorrelation function, as calculated using the first-order Legendre polynomial, for selected systems at two temperatures is shown in Figure 10. The relaxation presents a complex decay, consisting of at least two processes as observed from the data at 400 K (where a more rapid decorrelation occurs); a first decay at approximately

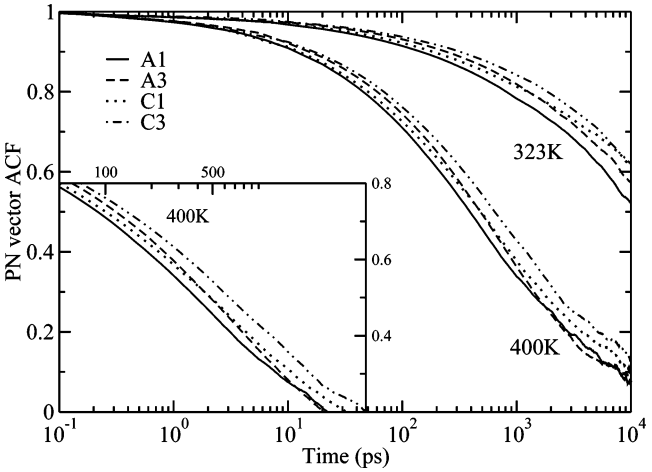


**Figure 10.** Autocorrelation function of the unit vector along the phosphorus−nitrogen direction of the lipid headgroups for selected systems at two temperatures, 323 and 400 K. The inset presents an enlarged area of the data at 400 K. Continuous lines are calculated from pure DPPC bilayers. Dashed lines correspond to systems with trehalose, and dotted lines represent systems with a high cholesterol content. Dashed−double dotted lines are used to display the effect of the presence of both sugar and sterol molecules.

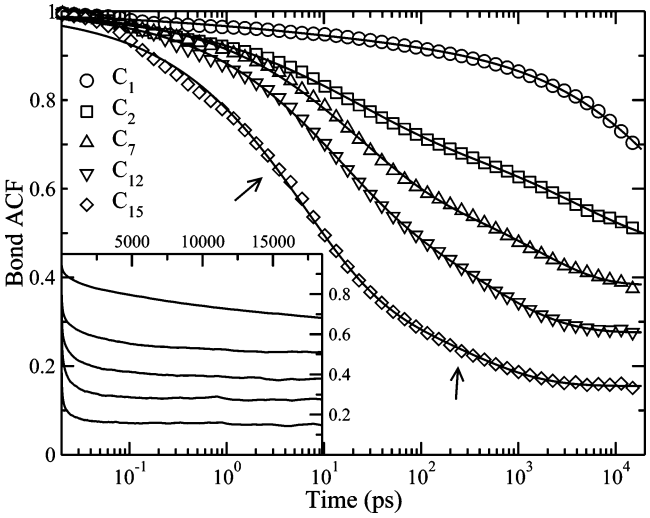


**Figure 11.** Bond autocorrelation functions for selected carbon atoms along the lipid Sn−1 tails at 323 K. Points are data from simulations, and lines are fits with eq 3. The inset displays the simulation data on a linear time scale where the plateau values of the time correlation functions are apparent.

100 ps, corresponding to vector reorientations, is followed by a second process at times longer than 1 ns, associated with whole lipid motions. At 323 K, the dynamics of the system are considerably slower, and only a limited part of the decay can be extracted even at times as long as 20 ns. Despite the progressively larger statistical error involved in the calculation of dynamic properties (depending on time intervals), there is an apparent difference between the changes imposed by the sugar and by the sterol on the dynamics of the hydrophilic part of the membrane.

Trehalose induces a considerable decrease of the rate of reorientation in the short time regime, as expressed by the slower decrease of the dashed lines. This ability of the sugar to depress the fast motions of biomolecules has been studied in a range of systems by both experimental and simulation methods; it is also supported by our simulations of hydrated DPPC bilayers. Experiments on DPPC−trehalose systems using FTIR have suggested a decrease of high-frequency vibrations.[9] Our simulations show that even the reorientation of the vector is significantly decelerated in the high-frequency regime. At long times and high temperatures, the life span of interactions between sugar molecules and lipid headgroups can be shorter than the time explored by our simulations,[24] resulting in similar dynamics for the A1 and A3 systems. At low temperatures, trehalose molecules are able to bind to the lipids for much longer times, thereby leading to dynamics slower than those for the pure DPPC system, even at the longest time sampled by our simulations.

The changes imposed by the cholesterol molecules become increasingly apparent when the long-time behavior of the autocorrelation functions is examined. The headgroup mobility is almost unaffected in the short-time regime by the presence of the sterols in the hydrophobic part of the membrane. The second part of the decay, which corresponds to whole lipid motions, is altered considerably. Cholesterol decreases the diffusion of the lipids by acting on the tails of the molecules and consequently affects greatly the fluidity of the bilayer. The additive character of the presence of both components in the lipid systems is displayed by the dashed−double dotted lines, which present a major decrease of mobility at all time scales studied and at both high and low temperatures.

The above findings correspond to the dynamics of the lipid headgroups but do not provide any information of the mobility in the hydrophobic regime of the membrane. The dynamics of tails exhibit an even more complex dynamic behavior, consisting of a number of relaxation processes appearing at different characteristic times that vary along the position along the lipid tail. Experimentally, NMR with specific labeling has provided evidence of very fast motions corresponding to trans−gauche isomerization at rates in the picosecond regime. Overall, rotational modes occur on longer time scales (nanoseconds). Long-range collective motions also arise in lipid bilayers.[78,79] Simulations have supported the existence of a combination of fast and slow motions, in accordance with experiment, with correlation times that display a clear dependence on the location along the lipid chains.[75,80−82] To evaluate the different motions in the lipid tails in our simulations, the bond autocorrelation functions expressed by the first-order Legendre polynomial were calculated for all unit vectors along the bond connecting methylene groups in both Sn−1 and Sn−2 chains. The inset of Figure 11 presents simulation predictions as extracted from the A1 system at 323 K for specific positions along the Sn−1 tail of the lipids, starting from the first bond after the carbonyl group ($C_1$) to the last bond vector ($C_{15}$). It is found that the reorientation of the vectors decorrelates to a constant nonzero value after a few nanoseconds. This plateau is determined by the ability of the bonds to rotate over increasingly larger volumes by moving to the tail end, but it never decorrelates completely due to preferential orientation of the chain segments parallel to the membrane normal, as shown also in Figure 8. A complex dynamic behavior can be resolved by plotting the data on a logarithmic scale. Two apparent regimes are detected, as pointed by the two arrows in the figure: one corresponding to trans−gauche isomerizations at short times and a second corresponding to rotational diffusion around the lipid axes.[81,82] A noticeable finding is that no isomerization is found for the first bond whose dynamics are not described by alkane torsional conformations because of the presence of the carbonyl group.

Because of the complex dynamics of the lipid tails, the description of the data with a simple mathematical model is not straightforward. Simulation results have been analyzed in the past either by a sum of exponential functions and a plateau value or by stretched exponentials (also called Kohlrausch−

Williams−Watts (KWW) functions).[80,81] We found that the simulation curves can be described accurately by a sum of two stretched exponentials with a plateau value. A thorough inspection of the decorrelation shape for bonds close to the end of the tails reveals that a third decay could be present at short times below 1 ps; we chose not to include such a feature in our fitting procedure to avoid an increase in the adjustable parameters in our model function. In summary, the dynamics were described by a function of the form

$$P_1(t) = A_f \cdot \exp[(-t/\tau_f)]^{\beta_f} + A_s \cdot \exp[(-t/\tau_s)]^{\beta_s} + A_p \quad (3)$$

where subscript f corresponds to the fast part of the decay, s to the subsequent slower part, and p to the constant value of the plateau regime. The fits were constrained so that $0 < \beta < 1$ and $A_f + A_s + A_p = 1$. The resulting curves are shown by the continuous lines in Figure 11. As illustrated in the figure, a very good description is achieved by the model function. Our fits provide us with the amplitudes of the different parts of the decays $A$ and the mean relaxation times for the fast and slow motions, calculated analytically as $\tau_{mean} = (\tau/\beta)\Gamma(1/\beta)$ by integrating separately each of the KWW functions. The extracted $A_p$ values vary from 0.15 to 0.55 and follow a pattern similar to that of the carbon−deuterium order parameter. Cholesterol increases $A_p$ considerably, while a small decrease is observed for trehalose. A difference from the $S_{CD}$ graph is that $A_p$ appears to display an odd−even effect for the first carbon atoms, as observed in the carbon−carbon order parameter $S_{CC}$.[83,84] A decrease of the magnitude of this effect was clearly found in the presence of trehalose.

The mean characteristic times of the fast motions vary from 11 to 3 ps ($C_2$ to $C_{15}$) at 400 K and 80−10 ps at 323 K. The only noticeable difference between different systems is a slight increase in correlation times for systems containing either trehalose or cholesterol. A significant modification is detected for the amplitude of the decay at short times; a noticeable reduction is observed for bilayers containing cholesterol molecules. The sugar retains or increases the amplitudes extracted from the fits. The variation of $A_f$ along the lipid tails is displayed in Figure 12a and follows a dependence comparable to that of the isomerization rates for pure lipids reported in the literature.[80] Furthemore, the pattern displays an inverse relationship with the density profiles shown in Figure 3, supporting the local character of trans−gauche isomerizations and their dependence on free volume in the system.

The slow dynamics of the tails as depicted by the mean relaxation times are always decelerated in the presence of either the disaccharide or the sterol, ranging from 2 ns to 80 ps ($C_2$ to $C_{15}$) at 400 K and 10 ns to 800 ps at 323 K. The characteristic times for select systems are presented in Figure 12 at 400 K, where the rather slow part of the decay is well-resolved in the time window of our simulations. The origin of this effect is that cholesterol is located in the hydrophobic region and restricts rotational diffusion. Trehalose, although absent in the immediate vicinity of the lipid tails, interacts with headgroups and carbonyl groups, thereby giving rise to an increase in rotational correlation times. The increase of the mean characteristic times in the presence of trehalose at the concentrations studied here is considerably lower than that in the case of cholesterol, but the imposed modifications exhibit a definite additive character.

## IV. Conclusions

The effects of trehalose and cholesterol in the properties of lipid bilayers were studied through molecular simulations.

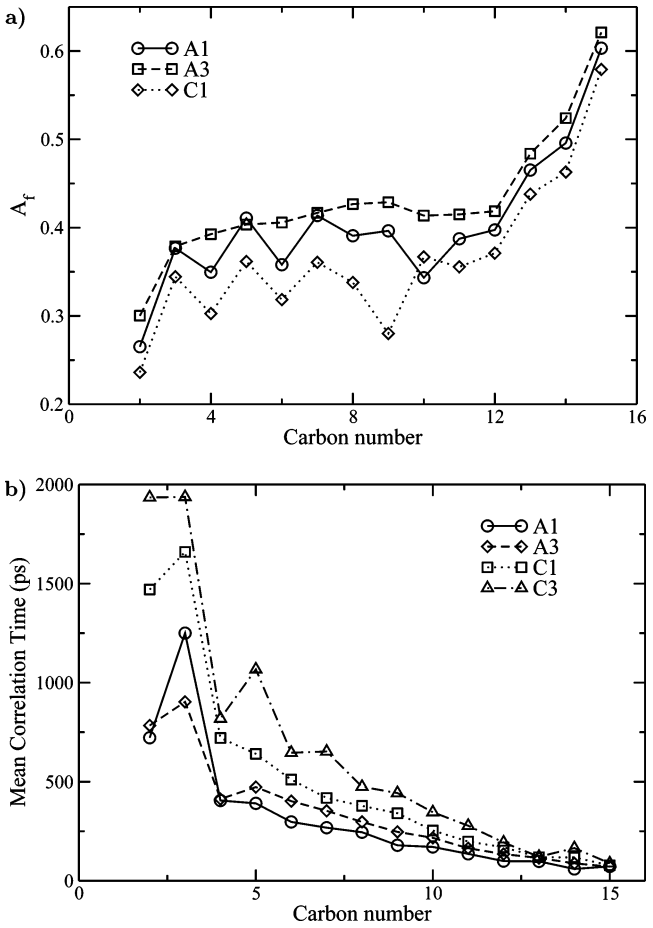


**Figure 12.** (a) Amplitude of fast motions at the Sn−1 chain for selected systems at 323 K. (b) Mean correlation times of the slow motions at the Sn−1 chain for selected systems at 400 K.

Trehalose is found to partition preferentially to the lipid headgroup region. In moderate concentrations, it alters the separation of the membrane constituents even in the presence of cholesterol, a finding that supports the protective character of the sugar in experiments with mammalian cells containing large amounts of cholesterol (e.g., red blood cells). As shown by predictions of the area per lipid, the gauche fraction of tail dihedral angles, and the carbon−deuterium order parameters, in all cases the disaccharide is at least as effective in systems with cholesterol as it is in pure bilayers. While the two components are located in different parts of the membrane, trehalose moderates the condensing effect induced by interactions of cholesterol with the phospholipids, presenting an additional mechanism to control the membrane properties.

A significant result of our study is that the dynamics of the bilayer are considerably modified. The slow rotational and translational modes of the membrane molecules are decelerated to a considerable extent. Such a phenomenon suggests that trehalose can inhibit changes in lateral organization of the bilayer components, which is vital in preventing leakage during preservation procedures. The decrease of motional rates imposed by cholesterol and trehalose at the hydrophilic part of the membrane is not concurrent. The sugar mainly reduces the high-frequency motions (shorter times), while the sterol effect is more apparent at lower frequencies (longer times). At the lipid tails, two different dynamic regimes are easily extracted. The amplitude of the fast motions follows a close dependence on free volume and is greatly altered by the presence of cholesterol, in contrast to trehalose. The mean correlation times for the slow motions associated with rotation and translation increase with

the addition of either trehalose or cholesterol, providing a clear indication of restricted long-range motion of the membrane constituents in these multicomponent biological systems.

**Acknowledgment.** This work is supported by the National Science Foundation. Partial support from the UW-MRSEC is gratefully acknowledged.

## References and Notes

(1) Strauss, G.; Hauser, H. *Proc. Natl. Acad. Sci. U.S.A.* **1986**, *83*, 2422.
(2) Nakagaki, M.; Nagase, H.; Ueda, H. *J. Membr. Sci.* **1992**, *73*, 173.
(3) Benaroudj, N.; Lee, D. H.; Goldberg, A. L. *J. Biol. Chem.* **2001**, *276*, 24261.
(4) Crowe, J. H.; Crowe, L. M. *Nat. Biotechnol.* **2000**, *18*, 145.
(5) Crowe, J. H.; Crowe, L. M.; Oliver, A. E.; Tsvetkova, N.; Wolkers, W.; Tablin, F. *Cryobiology* **2001**, *43*, 89.
(6) Bryant, G.; Koster, K. L.; Wolfe, J. *Seed Sci. Res.* **2001**, *11*, 17.
(7) Zavaglia, A. G.; Tymczyszyn, E.; Antoni, G. D.; Disalvo, E. A. *J. Appl. Microbiol.* **2003**, *95*, 1315.
(8) Crowe, J. H.; Oliver, A. E.; Tablin, F. *Integr. Comp. Biol.* **2002**, *42*, 497.
(9) Crowe, J. H.; Crowe, L. M.; Chapman, D. *Science* **1984**, *223*, 701.
(10) Crowe, J. H.; Hoekstra, F. A.; Crowe, L. M. *Annu. Rev. Physiol.* **1992**, *54*, 579.
(11) Hershkovitz, N.; Oren, A.; Cohen, Y. *Appl. Environ. Microbiol.* **1991**, *57*, 645.
(12) Crowe, J. H.; Carpenter, J. F.; Crowe, L. M. *Annu. Rev. Physiol.* **1998**, *60*, 73.
(13) Wolfe, J.; Bryant, G. *Cryobiology* **1999**, *39*, 103.
(14) Koster, K. L.; Lei, Y. P.; Anderson, M.; Martin, S.; Bryant, G. *Biophys. J.* **2000**, *78*, 1932.
(15) Johnston, D. S.; Coppard, E.; Parera, G. V.; Chapman, D. *Biochemistry* **1984**, *23*, 6912.
(16) Lee, C. W. B.; Waugh, J. S.; Griffin, R. G. *Biochemistry* **1986**, *25*, 3737.
(17) Lee, C. W. B.; Gupta, S. K. D.; Mattai, J.; Shipley, G. G.; Abdel-Mageed, O. H.; Makriyannis, A.; Griffin, R. G. *Biochemistry* **1989**, *28*, 5000.
(18) Lambruschini, C.; Relini, A.; Ridi, A.; Cordone, L.; Gliozzi, A. *Langmuir* **2000**, *16*, 5467.
(19) Luzardo, M.; Amalfa, F.; Nuñez, A. M.; Díaz, S.; Biondi de Lopez, A. C.; Disalvo, E. A. *Biophys. J.* **2000**, *78*, 2452.
(20) Hays, L. M.; Crowe, J. H.; Wolkers, W.; Rudenko, S. *Cryobiology* **2001**, *42*, 88.
(21) Conrad, P.; de Pablo, J. J. *J. Phys. Chem. A* **1999**, *103*, 4049.
(22) Ekdawi-Sever, N. C.; Conrad, P. B.; de Pablo, J. J. *J. Phys. Chem. A* **2001**, *105*, 734.
(23) Ekdawi-Sever, N. C.; de Pablo, J. J.; Feick, E.; von Meerwall, E. *J. Phys. Chem. A* **2003**, *107*, 936.
(24) Sum, A. K.; Faller, R.; de Pablo, J. J. *Biophys. J.* **2003**, *85*, 2830.
(25) Pereira, C. S.; Lins, R. D.; Chandrasekhar, I.; Freitas, L. C. G.; Hünenberger, P. H. *Biophys. J.* **2004**, *86*, 2273.
(26) Villarreal, M. A.; Díaz, S. B.; Disalvo, E. A.; Montich, G. G. *Langmuir* **2004**, *20*, 7844.
(27) Ricker, J. V.; Tsvetkova, N. M.; Wolkers, W. F.; Leidy, C.; Tablin, F.; Longo, M.; Crowe, J. H. *Biophys. J.* **2003**, *84*, 3045.
(28) Ohtake, S.; Schebor, C.; Palacek, S. P.; de Pablo, J. J. *Biochim. Biophys. Acta* **2005**, *1713*, 57.
(29) Beattie, G. M.; Crowe, J. H.; Lopez, A. D.; Cirulli, V.; Ricordi, C.; Hayek, A. *Diabetes* **1997**, *46*, 519.
(30) Beattie, G. M.; Leibowitz, G.; Lopez, A. D.; Levine, F.; Hayek, A. *Cell Transplant.* **2000**, *9*, 431.
(31) Guo, N.; Puhlev, I.; Brown, D. R.; Mansbridge, J.; Levine, F. *Nat. Biotechnol.* **2000**, *18*, 168.
(32) Puhlev, I.; Guo, N.; Brown, D. R.; Levine, F. *Cryobiology* **2001**, *42*, 207.
(33) Mussauer, H.; Sukhorukov, V. L.; Zimmermann, U. *Cytometry* **2001**, *45*, 161.
(34) Reuss, R.; Ludwig, J.; Shirakashi, R.; Ehrhart, F.; Zimmermann, H.; Schneider, S.; Weber, M. M.; Zimmermann, U.; Schneider, H.; Sukhorukov, V. L. *J. Membr. Biol.* **2004**, *200*, 67.
(35) Wolkers, W. F.; Walker, N. J.; Tablin, F.; Crowe, J. H. *Cryobiology* **2001**, *42*, 79.
(36) Wolkers, W. F.; Tablin, F.; Crowe, J. H. *Comp. Biochem. Physiol., A* **2002**, *131*, 535.
(37) Nie, Y.; de Pablo, J. J.; Palecek, S. P. *Biotechnol. Bioeng.* **2005**, *92*, 79.
(38) Erdag, G.; Eroglu, A.; Morgan, J. R.; Toner, M. *Cryobiology* **2002**, *44*, 218.
(39) Ji, L.; de Pablo, J. J.; Palecek, S. P. *Biotechnol. Bioeng.* **2004**, *88*, 299.
(40) Satpathy, G. R.; Török, Z.; Bali, R.; Dwyre, D. M.; Little, E.; Walker, N. J.; Tablin, F.; Crowe, J. H.; Tsvetkova, N. M. *Cryobiology* **2004**, *49*, 123.
(41) Yeagle, P. L. *The Membranes of Cells*; Academic Press, Inc.: San Diego, 1993.
(42) Tu, K.; Klein, M. L.; Tobias, D. J. *Biophys. J.* **1998**, *75*, 2147.
(43) Smondyrev, A. M.; Berkowitz, M. L. *Biophys. J.* **1999**, *77*, 2075.
(44) Pasenkiewicz-Gierula, M.; Róg, T.; Kitamura, K.; Kusumi, A. *Biophys. J.* **2000**, *78*, 1376.
(45) Chiu, S. W.; Jakobsson, E.; Scott, H. L. *Biophys. J.* **2001**, *80*, 1104.
(46) Chiu, S. W.; Jakobsson, E.; Scott, H. L. *J. Chem. Phys.* **2001**, *114*, 5435.
(47) Smondyrev, A. M.; Berkowitz, M. L. *Biophys. J.* **2001**, *80*, 1649.
(48) Chiu, S. W.; Jakobsson, E.; Mashl, R. J.; Scott, H. L. *Biophys. J.* **2002**, *83*, 1842.
(49) Hofsäss, C.; Lindahl, E.; Edholm, O. *Biophys. J.* **2003**, *84*, 2192.
(50) Jedlovszky, P.; Mezei, M. *J. Phys. Chem. B* **2003**, *107*, 5311.
(51) Jedlovszky, P.; Mezei, M. *J. Phys. Chem. B* **2003**, *107*, 5322.
(52) Jedlovszky, P.; Medvedev, N. N.; Mezei, M. *J. Phys. Chem. B* **2004**, *108*, 465.
(53) Pandit, S. A.; Bostick, D.; Berkowitz, M. L. *Biophys. J.* **2004**, *86*, 1345.
(54) Falck, E.; Patra, M.; Karttunen, M.; Hyvönen, M. T.; Vattulainen, I. *Biophys. J.* **2004**, *87*, 1076.
(55) Falck, E.; Patra, M.; Karttunen, M.; Hyvönen, M. T.; Vattulainen, I. *J. Chem. Phys.* **2004**, *121*, 12676.
(56) McMullen, T. P. W.; Lewis, R. N. A.; McElhaney, R. N. *Biochemistry* **1993**, *32*, 516.
(57) van Gunsteren, W. F.; Billeter, S. R.; Eising, A. A.; Hünenberger, P. H.; Krüger, P.; Mark, A. E.; Scott, W. R. P.; Tironi, I. G. *Biomolecular Simulation: The GROMOS Manual and User Guide*; Hochschuleverlag AG an der ETH: Zürich, Switzerland, 1996.
(58) Nath, S. K.; Escobedo, F. A.; de Pablo, J. J. *J. Chem. Phys.* **1998**, *108*, 9905.
(59) Nath, S. K.; de Pablo, J. J. *Mol. Phys.* **2000**, *98*, 231.
(60) Nath, S. K.; Banaszak, B. J.; de Pablo, J. J. *J. Chem. Phys.* **2001**, *114*, 3612.
(61) Höltje, M.; Förster, T.; Brandt, B.; Engels, T.; von Rybinski, W.; Höltje, H.-D. *Biochim. Biophys. Acta* **2001**, *1511*, 156.
(62) Damm, W.; Frontera, A.; Tirado-Rives, J.; Jorgensen, W. L. *J. Comput. Chem.* **1997**, *18*, 1955.
(63) Berendsen, H. J. C.; Postma, J. P. M.; van Gunsteren, W. F.; Hermans, J. Interaction models for water in relation to protein hydration. In *Intermolecular Forces*; Pullman, B., Ed.; Reidel: Dordrecht, The Netherlands, 1996.
(64) Lindahl, E.; Hess, B.; van der Spoel, D. *J. Mol. Model.* **2001**, *7*, 306.
(65) Berendsen, H. J. C.; van der Spoel, D.; van Drunen, R. *Comput. Phys. Commun.* **1995**, *91*, 43.
(66) Hess, B.; Bekker, H.; Berendsen, H. J. C.; Fraaije, J. G. E. M. *J. Comput. Chem.* **1997**, *18*, 1463.
(67) Essman, U.; Perela, L.; Berkowitz, M. L.; Darden, T.; Lee, H.; Pedersen, L. G. *J. Chem. Phys.* **1995**, *103*, 8577.
(68) Berendsen, H. J. C.; van Gunsteren, W. F.; Postma, J. P. M.; DiNola, A.; Haak, J. R. *J. Chem. Phys.* **1984**, *81*, 3684.
(69) Hønger, T.; Mortensen, K.; Ipsen, J. H.; Lemmich, J.; Bauer, R.; Mouritsen, O. G. *Phys. Rev. Lett.* **1994**, *72*, 3911.
(70) Lemmich, J.; Mortensen, K.; Ipsen, J. H.; Hønger, T. H.; Bauer, R.; Mouritsen, O. G. *Phys. Rev. Lett.* **1995**, *75*, 3958.
(71) Nagle, J. F.; Petrache, H. I.; Gouliaev, N.; Tristram-Nagle, S.; Liu, Y.; Suter, R. M.; Gawrisch, K. *Phys. Rev. E* **1998**, *58*, 7769.
(72) Pabst, G.; Katsaras, J.; Raghunathan, V. A.; Rappolt, M. *Langmuir* **2003**, *19*, 1716.
(73) Nagle, J. F.; Tristram-Nagle, S. *Biochim. Biophys. Acta* **2000**, *1469*, 159.
(74) Richter, F.; Finegold, L.; Rapp, G. *Phys. Rev. E* **1999**, *59*, 3483.
(75) Tieleman, D. P.; Marrink, S. J.; Berendsen, H. J. C. *Biochim. Biophys. Acta* **1997**, *1331*, 235.
(76) Seelig, A.; Seelig, J. *Biochemistry* **1974**, *13*, 4839.
(77) Petrache, H. I.; Dodd, S. W.; Brown, M. F. *Biophys. J.* **2000**, *79*, 3172.
(78) Meier, P.; Ohmes, E.; Kothe, G. *J. Chem. Phys.* **1986**, *85*, 3598.
(79) Weisz, K.; Gröbner, G.; Mayer, C.; Stohrer, J.; Kothe, G. *Biochemistry* **1992**, *31*, 1100.
(80) Venable, R. M.; Zhang, Y.; Hardy, B. J.; Pastor, R. W. *Science* **1993**, *262*, 223.
(81) Lindahl, E.; Edholm, O. *J. Chem. Phys.* **2001**, *115*, 4938.
(82) Moore, P. B.; Lopez, C. F.; Klein, M. L. *Biophys. J.* **2001**, *81*, 2484.
(83) Douliez, J.-P.; Léonard, A.; Dufourc, E. J. *J. Phys. Chem.* **1996**, *100*, 18450.
(84) Douliez, J.-P.; Ferrarini, A.; Dufourc, E.-J. *J. Chem. Phys.* **1998**, *109*, 2513.